

# Design of a Bidirectional Metamaterial Spacer at 2.45 GHz

M. Imbert, P.J. Ferrer, J.M. González-Arbesú, and J. Romeu

AntennaLab – TSC, Universitat Politècnica de Catalunya (UPC)

c/ Jordi Girona, 1-3, D3-212 08034 Barcelona – {pj.ferrer, jmgonzalez}@tsc.upc.edu

**Abstract**— A bidirectional metamaterial spacer composed by Spiral Resonators (SRs) and metal strips has been designed, simulated, fabricated, and tested to operate like an artificial magnetic conductor (AMC) reflector at 2.45 GHz. A prototype of the new metamaterial spacer has been used to decorrelate two closely spaced monopole antennas achieving a good isolation and matching over a wide frequency range. This design could be used to develop a more compact multi-antenna Wi-Fi (IEEE 802.11b/g) router.

## I. INTRODUCTION

Metamaterials and other resonating structures have been widely used to isolate closely spaced antennas [1]-[2]. In [3], a bidirectional artificial magnetic conductor (AMC) spacer was designed to decouple and decorrelate two monopoles.

In this work, a metamaterial spacer composed by spiral resonators (SR) and strips has been designed, simulated, fabricated and tested to achieve a bidirectional AMC behavior around 2.45 GHz (ISM band) with enhanced isolation. The fabricated design can also be used as a compact antenna system for wireless 802.11b/g network applications.

## II. METAMATERIAL SPACER DESIGN AND SIMULATION

In order to improve the isolation level of a two-antenna system [3], and in turn, reduce the electrical thickness of the spacer, we have carried out three variations in the initial design of the spiral resonator [4], in order to operate at 2.45 GHz. Fundamentally, when a linearly polarized incident electric field plane wave impinges a SR orthogonally to the axis of the SR, we get a PMC-like response on one side and a PEC-like response on the other one. Then, a bidirectional PMC behavior could be obtained by putting together in the same axis two (or more) resonators with the PMC side facing outwards.

We initially assume the same SR model (2-turn square-shaped Greek key spiral) with the same dimensions as in [4]. That SR design operates around 2.61 GHz. Thus, we have studied and optimized this design in three steps in order to finally operate at 2.45 GHz, while isolation is enhanced.

### A. First variation

We increase the SR strip length giving half more turn on the SR's arm. With this action, we shift the PMC response (phase ( $S_{11}$ ) =  $0^\circ$ ) at 2.48 GHz, while maintaining the same thickness. The HFSS simulation results of this design are shown in Fig. 1, where the magnitude and phase of the  $S_{11}$  and the magnitude of the  $S_{21}$  parameters are plotted. A sketch of the new bidirectional AMC unit cell is shown in the inset in

Fig. 1. The main dimensions of each SR are the following: major side of 5.6 mm, strip width of 0.6 mm, and gap width of 0.4 mm. The inner gap between the two SRs is of 1 mm. The SRs are made of copper with 18  $\mu\text{m}$  of thickness, and they are etched on Rogers 4003C dielectric substrate ( $\epsilon_r = 3.38$ ,  $\tan \delta = 0.0027$ ) with a thickness of 0.8 mm. The unit cell dimensions are  $13 \times 6 \times 4 \text{ mm}^3$  ( $t \times h \times g$ ).

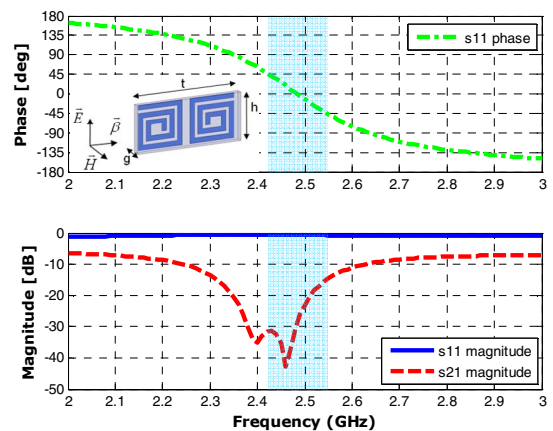


Fig. 1: Simulated phase (top) and magnitude (bottom) results of  $S_{11}$  and  $S_{21}$  parameters of the first design. The sketch of the unit cell is shown in the inset. The shaded band identifies the  $\pm 45^\circ$  fractional bandwidth (PMC behavior).

With this design, we have improved the electrical thickness from  $\lambda/8.8$  to  $\lambda/9.3$  because the operational frequency has been shifted to a lower value. At the resonant frequency, the magnitude of  $S_{11}$  is -0.63 dB ( $S_{22}$  parameter is not plotted due to the symmetry in the design), and the  $\pm 45^\circ$  fractional bandwidth (PMC behavior) is of 5.22%. The magnitude of  $S_{21}$  (isolation level) is -43 dB at 2.46 GHz. In order to improve the isolation and reduce the electrical thickness we have carried out a second variation in the design keeping the first step.

### B. Second variation

We reduce the thickness of design by overlapping the two SRs in  $t$  (horizontal) and  $h$  (vertical) dimensions, as it is seen in the sketch of the unit cell in Fig. 2. Note that, the interior gap between the two SRs is eliminated (reducing the thickness) and, moreover, due to the periodic boundary conditions (PBC), the design has a vertical continuity, overlapping the top and bottom arms of each spiral. With this variation we obtain a vertical continuity of the central common strip shared for the spirals that performs a better

isolation level. The resultant new unit cell dimensions are  $11.4 \times 5 \times 4 \text{ mm}^3$  ( $t \times h \times g$ ).

The HFSS simulation results of this second design are shown in Fig. 2. It is shown that the phase of the reflection coefficient  $S_{11}$  crosses  $0^\circ$  (PMC performance) at 2.63 GHz. The new thickness is 11.4 mm, improving the electrical thickness from  $\lambda/9.3$  to  $\lambda/10$ , not too smaller because we reduce physical dimensions but the frequency is now shifted to a higher value. At the resonant frequency, the magnitude of  $S_{11}$  is  $-0.53 \text{ dB}$ , and the  $\pm 45^\circ$  fractional bandwidth is improved up to 7.60%. The magnitude of  $S_{21}$  is  $-16 \text{ dB}$  at 2.63 GHz. It is shown that a  $-20 \text{ dB}$  of isolation has been achieved across a wide frequency band, in comparison of  $-10 \text{ dB}$  of general trend of the previous design. Moreover, there is a mismatch between the  $0^\circ$  phase crossing of  $S_{11}$  parameter and the minimum value of the isolation (magnitude of  $S_{21}$  parameter). This mismatch causes that, at the resonant frequency (2.63 GHz, far from desired 2.45 GHz), we get only  $-16 \text{ dB}$  of isolation while the minimum value of isolation ( $-49 \text{ dB}$ ) is obtained at 2.49 GHz.

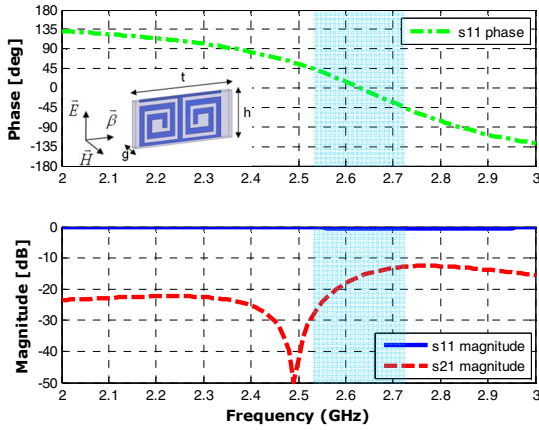


Fig. 2: Simulated phase (top) and magnitude (bottom) results of  $S_{11}$  and  $S_{21}$  parameters of the second design. The sketch of the unit cell is shown in the inset.

### C. Third variation

As mentioned earlier, the objective of this work is achieve a better isolation level while preserving the PMC condition (at 2.45 GHz) to a good reflection of the incident plane wave. In order to correct the mismatch, we introduce a third variation in the design. We use two additional copper strips, located orthogonally in each side of the original metamaterial slab, as it is seen in the sketch of Fig. 3. These additional strips are continuous in the horizontal dimension because of the PBC approximation used in the simulation (crossing side by side the unit cell), and there is a vertical discontinuity between them. The vertical dimension of each strip is of 4.2 mm, with a gap of 0.8 mm between two consecutive strips. The metal strips are placed at 1 mm from the beginning of each spiral resonator increasing the total thickness of the structure to 12.6 mm. With this action we would shift to a lower frequency the  $0^\circ$  phase crossing of  $S_{11}$  parameter.

The HFSS simulation results of this third design are shown in Fig. 3. A sketch of the new bidirectional AMC unit cell can be seen in the inset in Fig. 3. It is shown that the phase of the reflection coefficient  $S_{11}$  crosses  $0^\circ$  (PMC performance) at 2.42 GHz. At this resonant frequency the magnitude of  $S_{11}$  is  $-0.54 \text{ dB}$ , and a bandwidth of 170 MHz ( $\pm 45^\circ$  fractional bandwidth is of 7.02 %). The magnitude of  $S_{21}$  has a minimum value of  $-70 \text{ dB}$  at 2.45 GHz, improving about 20 dB with respect to the second design. Moreover, a  $-20 \text{ dB}$  level is achieved across the entire plotted band. The new electrical thickness is  $\lambda/9.84$ . With this third design, the reflection phase of  $S_{11}$  (PMC performance) and the minimum isolation are well matched around 2.45 GHz, as we desired.

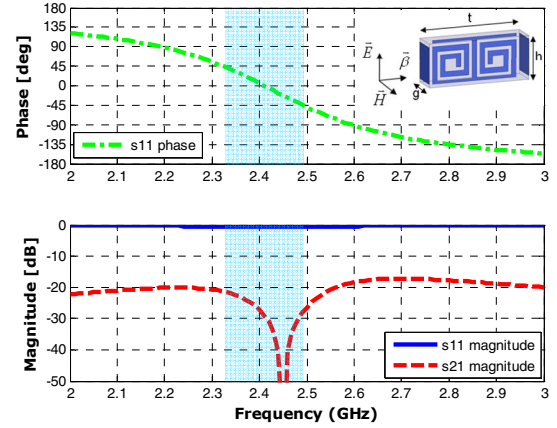


Fig. 3: Simulated phase (top) and magnitude (bottom) results of  $S_{11}$  and  $S_{21}$  parameters of the final design. The sketch of the unit cell is shown in the inset.

## III. FABRICATION AND MEASUREMENTS

### A. Fabrication of the Metamaterial Spacer

A metamaterial spacer, based on the third bidirectional AMC design, has been fabricated at our facilities using standard photo-etching techniques. The SRs are etched on Rogers RO4003C substrate, with a substrate thickness of 0.8 mm. The AMC spacer is composed of 15 dielectric strips of 5 cm of length; each strip contains 8 SRs. A nylon rod and some nylon rings are used to hold and maintain at a fixed separation (i.e. 4 mm) all the strips with SRs. The outer slab that contains 8 copper strips has also been etched on a Rogers RO4003C substrate with a thickness of 0.5 mm. The whole spacer has the width-height-thickness dimensions of  $60 \text{ mm} \times 50 \text{ mm} \times 12.6 \text{ mm}$  ( $0.49\lambda_{2.45\text{GHz}} \times 0.41\lambda_{2.45\text{GHz}} \times 0.1\lambda_{2.45\text{GHz}}$ ). A photograph of the AMC spacer prototype is shown in Fig. 4.

A two-monopole antenna system on an aluminum ground plane has also been fabricated to test the performance of the designed AMC spacer. The ground plane has a size of  $100 \text{ mm} \times 100 \text{ mm}$  ( $0.82\lambda_{2.45\text{GHz}} \times 0.82\lambda_{2.45\text{GHz}}$ ) and a thickness of 3 mm. These reduced size dimensions are similar to those of commercial Wi-Fi router case. The ground plane allows seven different distances (18, 24, 30, 35, 40, 50 and 60 mm) between the monopoles.

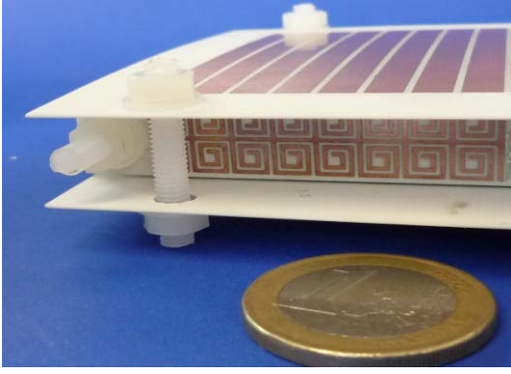


Fig. 4: Fabricated bidirectional AMC spacer composed by SRs and metal strips.

The two monopoles are formed from the extension of two SMA coaxial connectors. The monopoles are made of aluminum wire with a length of 29.5 mm and a diameter of 0.8 mm, in order to be matched at 2.45 GHz. A photograph of the fabricated ground plane with the two monopoles is shown in Fig. 5.

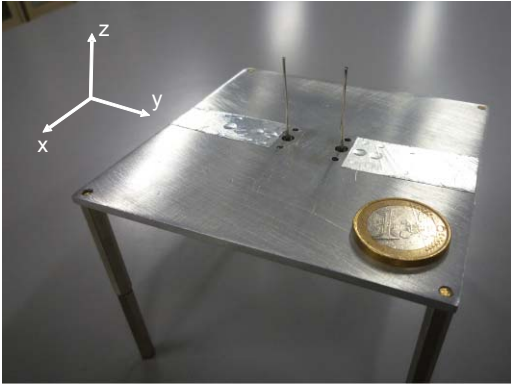


Fig. 5: Fabricated two-monopole antenna system over aluminum ground plane. This ground plane allows different distances between the monopoles.

### B. S-parameter Measurements

The performance of the fabricated AMC spacer together with the two-monopole system has been measured with an Agilent E8362 network analyzer from 2 to 3 GHz. The measurement setup is shown in Fig. 6.

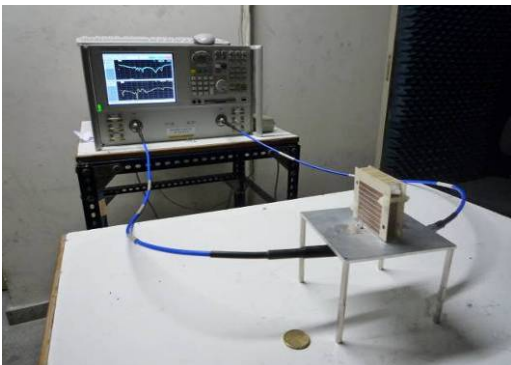


Fig. 6: Measurement setup for the two-monopole antenna system over a ground plane with the designed bidirectional AMC spacer with an Agilent E8362 network analyzer.

The magnitudes of the  $S_{11}$  and  $S_{21}$  parameters are plotted, for the cases of Air (no spacer) and AMC spacer between the monopoles, in Figs. 7, 8, and 9, for the distances of 18 mm, 24 mm, and 30 mm between the monopoles, respectively.

For a distance of 18 mm between antennas, a better matching level is achieved for each monopole in presence of the AMC spacer with respect to air case at 2.45 GHz, although this matching level is not achieved over the whole frequency band of interest (2.40-2.48 GHz). The magnitude of  $S_{11}$  parameter is improved from -9.6 dB to -11.8 dB at 2.45 GHz when using the AMC spacer, whereas the isolation  $S_{21}$  between monopoles is enhanced from -6.8 dB to -19.1 dB.

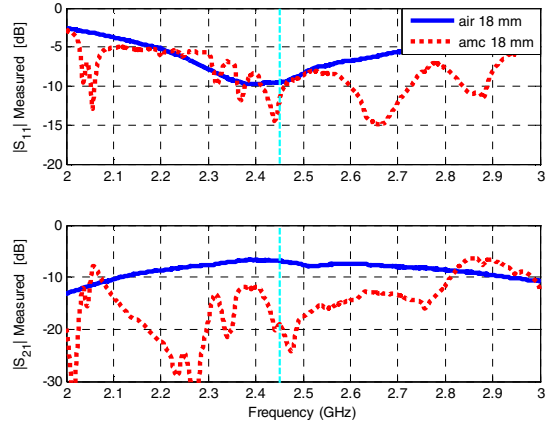


Fig. 7: Measured magnitudes of  $S_{11}$  and  $S_{21}$  parameters for the cases of Air (no spacer) and AMC spacer for a monopole separation of 18 mm.

For a monopole separation of 24 mm, it is shown that in presence of the AMC spacer a good matching level has been achieved over a wider frequency band (from 2.3 to 2.85 GHz). This is a great result considering the reduced dimensions of the ground plane. At 2.45 GHz, the magnitude of  $S_{11}$  parameter is improved from -10 dB (air case) to -17 dB (AMC spacer). The isolation between the antennas is enhanced from -8.5 dB to -21.4 dB.

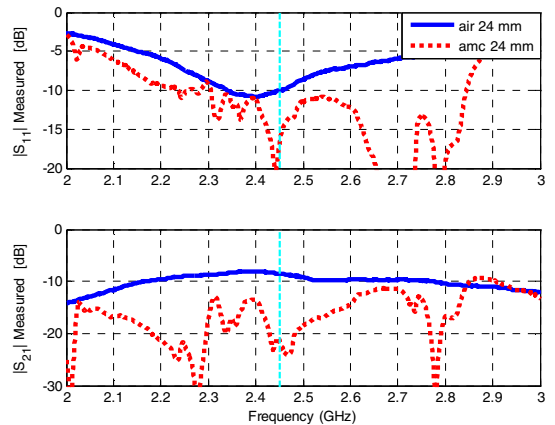


Fig. 8: Measured magnitudes of  $S_{11}$  and  $S_{21}$  parameters for the cases of Air (no spacer) and AMC spacer for a monopole separation of 24 mm.

As it is shown in Fig. 9, for a distance of 30 mm between the monopoles, the  $S_{11}$  and  $S_{21}$  parameters are also improved when using the AMC spacer. At 2.45 GHz, the magnitude of  $S_{11}$  is enhanced from -12 dB to value of -26 dB, achieving a wide matching band (2.2-2.8 GHz). The isolation is also improved at 2.45 GHz from -9.6 dB (no spacer) to -24.4 dB (with AMC surface).

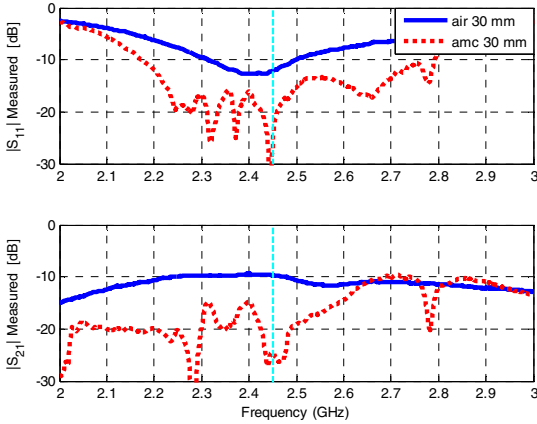


Fig. 9: Measured magnitudes of  $S_{11}$  and  $S_{21}$  parameters for the cases of Air (no spacer) and AMC spacer for a monopole separation of 30 mm.

After analyzing these results, it is observed that for the Air case, the matching and the isolation levels are slightly improved as the distance between the antennas increases, although the use of the designed metamaterial spacer significantly improves the results when no spacer is used. From now, 24 mm is considered as the reference separation between the monopoles antennas, because it represents the minimum separation between antennas in presence of the AMC spacer that provides matching and isolation enhancement at least over the whole frequency band of interest (2.4-2.48 GHz). This implies a trade-off between antenna system performance in presence of the AMC spacer and overall dimensions of the antenna system. In [5], it was shown that the performance of multiple antenna wireless systems (MIMO) is degraded by the mutual coupling between the antennas. With the designed AMC spacer, we have a compact antenna system with good performances in terms S-parameters (decoupling and matching) and this is potentially applicable to a compact multi-antenna Wi-Fi router system.

### C. Radiation Pattern Measurements

Good matching and isolation of an antenna system composed of two monopole antennas may also be reflected in quasi-orthogonal radiation patterns. Therefore, radiation patterns at 2.45 GHz have been measured in the D3-UPC anechoic chamber for a monopole separation of 24 mm. In the measurements, only one monopole is fed, whereas the other one has a  $50 \Omega$  load. The  $E$ -plane and  $H$ -plane cuts in the Air case (no spacer) and AMC spacer are plotted in Fig. 10. It is shown that in the  $E$ -plane cut, a monopole-like pattern has been obtained for the Air case, as expected. The insertion of the designed AMC spacer between the two monopoles slightly

reduces the back-radiation, tending to concentrate the energy into a half-space. In the  $H$ -plane cut, an almost omnidirectional pattern has been obtained for the Air case, whereas a back-radiation reduction is observed in presence of the AMC spacer. Although the measured back-radiation reduction is not as good as expected when compared with other designs that are found in literature, the isolation enhancement produced by the AMC spacer with respect to the Air case is confirmed.

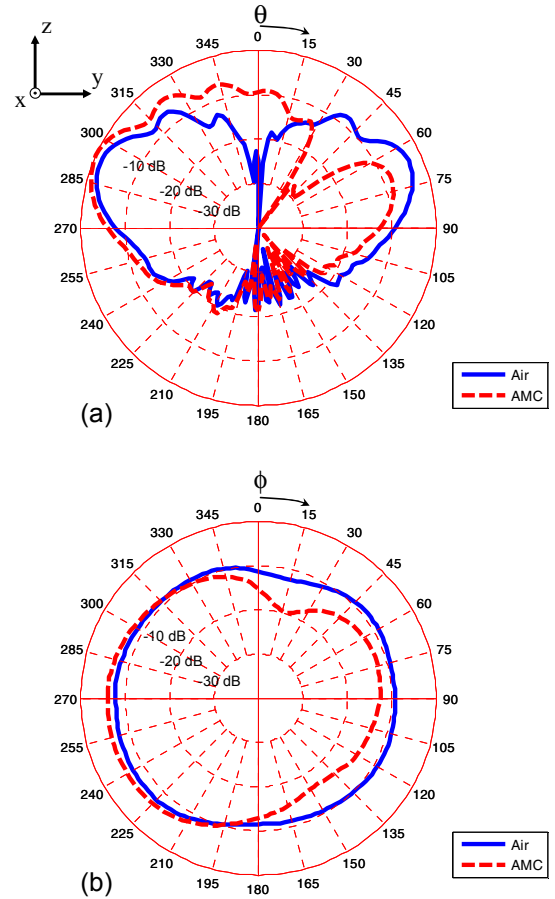


Fig. 10: Measured  $E$ -plane (a) and  $H$ -plane (b) radiation patterns at 2.45 GHz.

## IV. CONCLUSIONS

A bidirectional AMC spacer composed by SRs and metal strips has been designed, simulated, fabricated and tested. We have proposed three new variations in the original SR design introduced in [4] to achieve a higher isolation level, while keeping the PMC condition at the desired frequency (2.45 GHz). A prototype has been fabricated at our facilities using standard photo-etching techniques. The new bidirectional AMC spacer has been used to decouple two closely spaced monopoles obtaining a good performance in terms of S-parameters (matching level and isolation) and radiation patterns. It has been proved that it is possible reduce the distance (and volume) between two antennas, and hence, this prototype might be useful to design miniaturized and compact

multi-antenna systems for 802.11b/g applications operating at 2.45 GHz.

#### ACKNOWLEDGEMENTS

This work has been partially supported by the Spanish Interministerial Commission on Science and Technology (CICYT) under projects TEC2007-66698-C04-01/TCM, TEC2009-13897-C03-01 and CONSOLIDER CSD2008-00068.

#### REFERENCES

- [1] K. Buell, H. Mosallaei, and K. Sarabandi, "Metamaterial insulator enabled superdirective array", *IEEE Trans. Antennas Propagat.*, vol. 55, no. 4, pp. 1074-1085, Apr. 2007.
- [2] C. Chiu, C. Cheng, R. Murch, and C. Rowell, "Reduction of mutual coupling between closely-packed antenna elements", *IEEE Trans. Antennas Propagat.*, vol. 55, no. 6, pp. 1732-1738, Jun. 2007.
- [3] P.J. Ferrer, J.M. González-Arbesú, and J. Romeu, "Decorrelation of two closely spaced antennas with a metamaterial AMC surface", *Microw. Opt. Tech. Lett.*, vol. 50, no. 5, pp. 1414-1417, May 2008.
- [4] P.J. Ferrer, J.M. González-Arbesú, J. Romeu, and A. Cardama, "Bidirectional artificial magnetic reflectors at microwave frequencies", *Microw. Opt. Tech. Lett.*, vol. 49, no. 8, pp. 1949-1953, Aug. 2007.
- [5] G.J. Foschini and M.J. Gans, "On limits of wireless communications in a fading environment when using multiple antennas", *Wireless Personal Communications*, vol. 6, pp. 311-335, 1998.